Chapter 4

Quantum Dots: Phenomenology, Photonic and Electronic Properties, Modeling and Technology

Fredrik Boxberg and Jukka Tulkki

4.1 Introduction

4.1.1 What are they?

The research of microelectronic materials is driven by the need to tailor electronic and optical properties for specific component applications. Progress in epitaxial growth and advances in patterning and other processing techniques have made it possible to fabricate "artificial" dedicated materials for microelectronics.[1] In these materials, the electronic structure is tailored by changing the local material composition and by confining the electrons in nanometer-size foils or grains. Due to quantization of electron energies, these systems are often called quantum structures. If the electrons are confined by a potential barrier in all three directions, the nanocrystals are called quantum dots (QDs). This review of quantum dots begins with discussion of the physical principles and first experiments and concludes with the first expected commercial applications: single-electron pumps, biomolecule markers, and QD lasers.

In nanocrystals, the crystal size dependency of the energy and the spacing of discrete electron levels are so large that they can be observed experimentally and utilized in technological applications. QDs are often also called mesoscopic atoms or artificial atoms to indicate that the scale of electron states in QDs is larger than the lattice constant of a crystal. However, there is no rigorous lower limit to the size of a QD, and therefore even macromolecules and single impurity atoms in a crystal can be called QDs.

The quantization of electron energies in nanometer-size crystals leads to dramatic changes in transport and optical properties. As an example, Fig. 4.1 shows the dependence of the fluorescence wavelength on the dimensions and material composition of the nanocrystals. The large wavelength differences between the blue, green, and red emissions result here from using materials having different band gaps: CdSe (blue), InP (green), and InAs (red). The fine-tuning of the fluorescence emission within each color is controlled by the size of the QDs.

The color change of the fluorescence is governed by the "electron in a potential box" effect familiar from elementary text books of modern physics.[3] A simple potential box model explaining the shift of the luminescence wavelength is shown in the inset of Fig. 4.1. The quantization of electron states exists also in larger crystals, where it gives rise to the valence and conduction bands separated by the band gap. In bulk crystals, each electron band consists of a continuum of electron states. However, the energy spacing of electron states increases with decreasing QD size, and therefore the energy spectrum of an electron band approaches a set of discrete lines in nanocrystals.

As shown in Sec. 4.4, another critical parameter is the thermal activation energy characterized by $k_B T$. For the quantum effects to work properly in the actual devices, the spacing of energy levels must be large in comparison to $k_B T$, where k_B is Boltzmann's constant, and T the absolute temperature. For room-temperature operation, this implies that the diameter of the potential box must be at most a few nanometers.

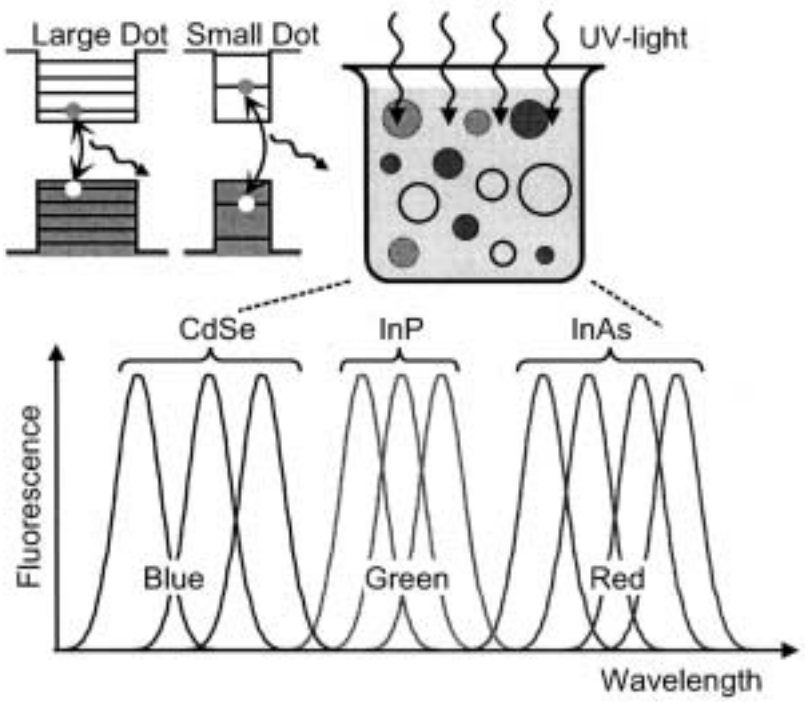

Figure 4.1 Nanocrystal quantum dots (NCQD) illuminated by UV-light emit light at a wavelength that depends both on the material composition and the size of the NCQDS. Large differences in the fluorescence wavelength result from different band gaps of the materials. Within each color (blue, green, and red) the wavelength is defined by the different sizes of the NCQDs.

In quantum physics, the electronic structure is often analyzed in the terms of the density of electron states (DOS). The prominent transformation from the continuum of states in a bulk crystal to the set of discrete electron levels in a QD is depicted in Fig. 4.2. In a bulk semiconductor [Fig. 4.2(a)], the DOS is proportional to the square root of the electron energy. In quantum wells (QWs) [see Fig. 4.2(b)], the electrons are restricted into a foil that is just a few nanometers thick. The QW DOS consists of a staircase, and the edge of the band (lowest electron states) is shifted to higher energies. However, in QDs the energy levels are discrete [Fig. 4.2(c)] and the DOS consists of a series of sharp (delta-function-like) peaks corresponding to the discrete eigenenergies of the electrons. Due to the finite life time of electronic states, the peaks are broadened and the DOS is a sum of Lorenzian functions. Figure 4.2(c) also depicts another subtle feature of QDs: In an experimental sample not all QDs are of the same size. Different sizes mean different eigenenergies; and the peaks in the DOS are accordingly distributed around some average energies corresponding to the average QD size. In many applications, the active device material contains a large ensemble of QDs. Their joint density of states then includes a statistical broadening characterized by a Gaussian function.[4] This broadening is

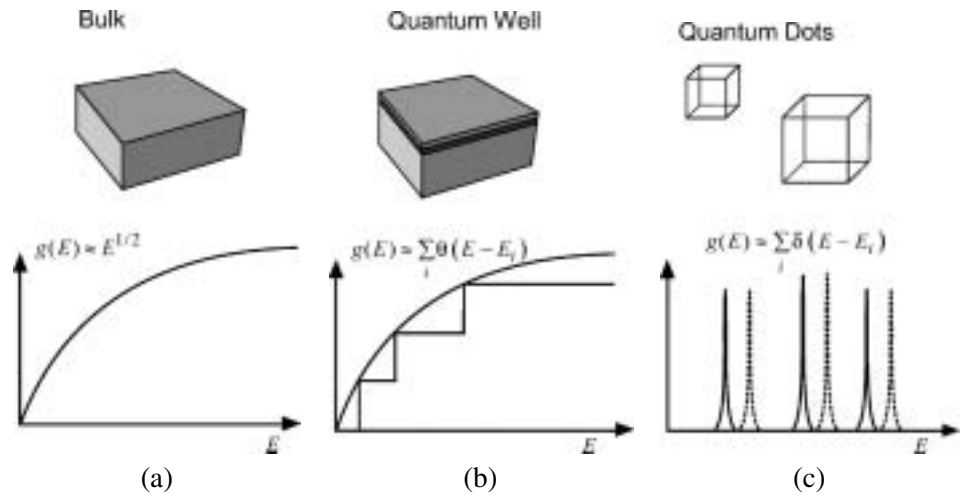

Figure 4.2 The density of electron states (DOS) in selected semiconductor crystals. The DOS of (a) bulk semiconductor, (b) quantum well, and (c) quantum dots.

often called inhomogeneous in distinction to the lifetime broadening, often called homogeneous broadening.[4]

4.1.2 History

Fabrication of QDs became possible because of the development of epitaxial growth techniques for semiconductor heterostructures. The prehistory of QDs began in the early 1970s with nanometer-thick foils called quantum wells. In QWs charge carriers (electrons and holes) become trapped in a few-nanometers-thick layer of wells, where the band gap is smaller than in the surrounding barrier layers. The variation of the band gap is achieved by changing the material composition of the compound semiconductor.[5]

The energy quantization in the optical absorption of a QW was first reported by Dingle et al.[6] in 1974. The photon absorption spectrum exhibits a staircase of discrete exciton resonances, whereas in the photon absorption of a bulk semiconductor only one exciton peak and the associated continuum is found. The transport properties of QW superlattices (periodic system of several QWs) were studied in the early 1970s by Esaki and Tsu.[7] The resonance tunneling effect and the related negative differential resistance was reported by Chang et al.[8] in 1974. These works began the exponential growth of the field during the 1970s; for a more complete list of references, see Bimberg et al.[4]

The experimental findings of Dingle et al.[6] were explained by the envelope wave function model that Luttinger and Kohn[9] developed for defect states in semiconductor single crystals. Resonant tunneling of electrons was explained in terms of quantum-mechanical transmission probabilities and Fermi distributions at source and drain contacts. Both phenomena were explained by the mesoscopic be-

havior of the electronic wave function,[9] which governs the eigenstates at the scale of several tens of lattice constants.

By the end of 1970, nanostructures could be fabricated in such a way that the mesoscopic variation of the material composition gave rise to the desired electronic potentials, eigenenergies, tunneling probabilities, and optical absorption. The quantum engineering of microelectronic materials was promoted by the Nobel prizes awarded in 1973 to L. Esaki for the discovery of the tunneling in semiconductors and in 1985 to K. von Klitzing et al.[10] for the discovery of the quantum Hall effect. Rapid progress was made in the development of epitaxial growth techniques: Molecular beam epitaxy[11] (MBE) and chemical vapor deposition[12] (CVD) made it possible to grow semiconductor crystals at one-monolayer accuracy.

In the processing of zero-dimensional (0D) and 1D structures, the development of electron beam lithography made it possible to scale down to dimensions of a few nanometers. Furthermore, the development of transmission electron microscopy (TEM), scanning tunneling microscopy (STM), and atomic force microscopy (AFM) made it possible to obtain atomic-level information of the nanostructures.

Figure 4.3 presents the discovery of level quantization in QDs reported by Ekimov and Onushenko[13] in 1984. The resonance structures are directly related to the energy quantization. One of the first measurements[14] of transport through a QD is shown in Fig. 4.4. In this case, the conductance resonance can be related to discrete charging effects that block the current unless appropriate QD eigenstates are accessible for electronic transport.

4.2 Fabrication

In the following, we limit our discussion to selected promising QD technologies including semiconductor nanocrystal QDs (NCQD), lithographically made QDs

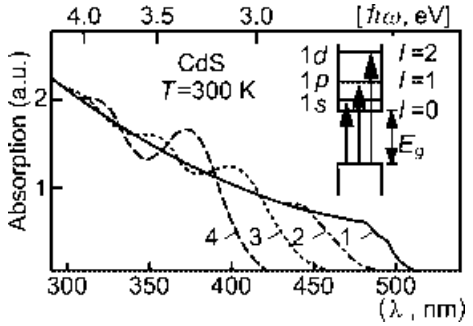

Figure 4.3 Photoabsorption by a set of CdS nanocrystals having different average radii as follows: (1) 38 nm, (2) 3.2 nm, (3) 1.9 nm, and (4) 1.4 nm. The inset marks the dipole transitions that are seen as resonances in absorption. The threshold of the absorption is blue-shifted when the size of the QD becomes smaller.[13]

(LGQDs), field-effect QDs (FEQDs), and self-assembled QDs (SAQDs). The main emphasis is on semiconductor QDs. Selected material parameters of the nanostructures are listed in Table 4.1.

Table 4.1 Selected room-temperature properties for the previously discussed materials.[32]

Material	Band gap (eV)	Electron mass (m_0)	Hole mass (m_0)	Permittivity (ε_0)
CdS	2.482(d)	0.165^a	$m^A_{p\perp} = 0.7$ $m^A_{p\parallel} = 5$	$\varepsilon^{\perp}(0) = 8.28$ $\varepsilon^{\perp}(\infty) = 5.23$ $\varepsilon^{\parallel}(0) = 8.73$ $\varepsilon^{\parallel}(\infty) = 5.29$
CdSe	1.738(d)	0.112^a	$m^A_{p\perp} = 0.45$ $m^A_{p\parallel} \geq 1$ $m^B_{p\perp} = 0.92$	$\varepsilon^{\perp}(0) = 9.29$ $\varepsilon^{\parallel}(0) = 10.16$ $\varepsilon(\infty) = 5.8$
GaAs	1.5192(d)	0.0635	$m_{hh[100]} = 0.33$ $m_{hh[111]} = 0.33$ $m_{lh[100]} = 0.090$ $m_{lh[111]} = 0.077$	$\varepsilon(0) = 12.80$ $\varepsilon(\infty) = 10.86$
InAs	0.4180(d)	0.023	$m_{hh} = 0.57$ $m_{[100]} = 0.35$ $m_{[111]} = 0.85$	$\varepsilon(0) = 14.5$ $\varepsilon(\infty) = 11.6$
InP	1.344(d)	0.073	$m_{hh} = 0.65$ $m_{lh} = 0.12$	$\varepsilon(0) = 12.61$ $\varepsilon(\infty) = 9.61$
Si	1.13(i)	$m_{\perp} = 0.1905^I$ $m_{\parallel} = 0.9163^I$	$m_{hh} = 0.537^I$ $m_{lh} = 0.153^I$	$\varepsilon = 11.9$

(^{I}The effective masses of Si are low temperature data $T = 4.2$ K). The low- and high-frequency permittivities are denoted by $\varepsilon(0)$ and $\varepsilon(\infty)$, respectively. The superscripts $^{\perp}$ and $^{\parallel}$ correspond to permittivities for the electric field perpendicular ($\overline{E} \perp c$) and parallel ($\overline{E} \parallel c$) with the c axis of the crystal.

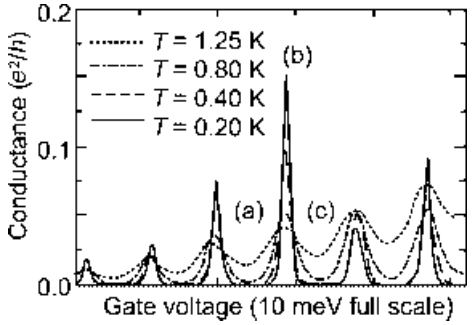

Figure 4.4 Conductance through a QD as a function of the gate voltage. Regions (a) and (c) indicate blocking of current by the Coulomb charging effect. In (b) electrons can tunnel from source to drain through empty electron states of the QD, thereby leading to a peak in the conductance. Note the rapid smearing of the resonance as the temperature increases.[14] (Reprinted with permission from Ref. 14, © 1991 The American Physical Society.)

4.2.1 Nanocrystals

A nanocrystal (NC) is a single crystal having a diameter of a few nanometers. A NCQD is a nanocrystal that has a smaller band gap than the surrounding material. The easiest way to produce NCQDs is to mechanically grind a macroscopic crystal. Currently NCQDs are very attractive for optical applications because their color is directly determined by their dimensions (see Fig. 4.1). The size of the NCQDs can be selected by filtering a larger collection of NCQDs or by tuning the parameters of a chemical fabrication process.

4.2.1.1 CdSe nanocrystals

Cadmium selenide (CdSe) and zinc selenide (ZnSe) NCQDs are approximately spherical crystalites with either wurtzite or zinc-blend structure. The diameter ranges usually between 10 and 100 Å. CdSe NCQDs are prepared by standard processing methods.[15] A typical fabrication procedure for CdSe NCQDs is described in Ref. 16. $Cd(CH_3)_2$ is added to a stock solution of selenium (Se) powder dissolved in tributylphosphine (TBP). This stock solution is prepared under N_2 in a refrigerator, while tri-*n*-octylphosphine oxide (TOPO) is heated in a reaction flask to 360°C under argon (Ar) flow. The stock solution is then quickly injected into the hot TOPO, and the reaction flask is cooled when the NCQDs of the desired size is achieved. The final powder is obtained after precipitating the NCQDs with methanol, centrifugation, and drying under nitrogen flow. The room-temperature quantum yield and photostability can be improved by covering the CdSe NCQDs with, e.g., cadmium sulphide (CdS).

By further covering the CdSe NCQDs by CdS, for example, the room-temperature quantum yield and photostability can be increased. The almost ideal crystal structure of a NCQD can be seen very clearly in the TEMs shown in Fig. 4.5.

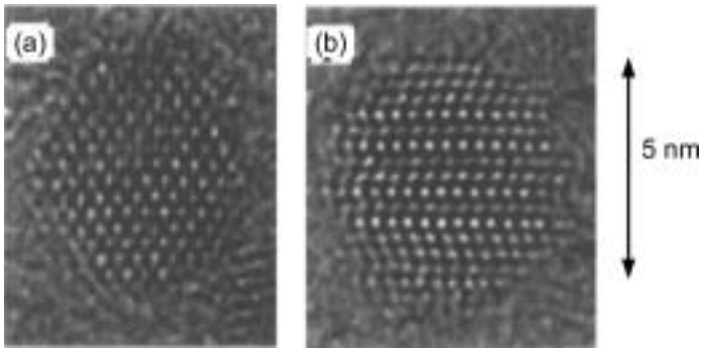

Figure 4.5 TEM images of CdSe/CdS core/shell NCQDs on a carbon substrate in (a) [001] projection and (b) [100] projection. Dark areas correspond to atom positions. The length bar at the right indicates 50 Å. (Reprinted with permission from Ref. 16, © 1997 American Chemical Society.)

Electron confinement in CdSe NCQDs is due to the interface between CdSe and the surrounding material. The potential barrier is very steep and at most equal to the electron affinity of CdSe. Even if the growth technique is fairly easy, it is very difficult to integrate single NCQDs into semiconductor chips in a controlled way, whereas the possibility to use them as biological labels or markers is more promising.[2]

4.2.1.2 Silicon nanocrystals

Silicon/silicon dioxide (Si/SiO_2) NCQDs are Si clusters completely embedded in insulating SiO_2.[17] They are fabricated by ion-implanting Si atoms into either ultrapure quartz or thermally grown SiO_2. The NCs are then formed from the implanted atoms under thermal annealing. The exact structure of the resulting NCQDs is not known. Pavesi et al.[17] reported successful fabrication of NCQDs with a diameter around 3 nm and a NCQD density of 2×10^{19} cm^{-3}. The high-density results[17] in an even higher light wave amplification (100 cm^{-1}) than for seven stacks of InAs QDs (70 to 85 cm^{-1}). The main photoluminescence peak was measured at $\lambda = 800$ nm. The radiative recombination in these QDs is not very well understood, but Pavesi et al. [17] suggested that the radiative recombinations take place through interface states. Despite the very high modal gain, it is very difficult to fabricate an electrically pumped laser structure of Si NCQD due to the insulating SiO_2.

4.2.2 Lithographically defined quantum dots

4.2.2.1 Vertical quantum dots

A vertical quantum dot (VQD) is formed by either etching out a pillar from a QW or a double barrier heterostructure[18,19] (DBH). Figure 4.6 shows the main steps in the fabrication process of a VQD. The AlGaAs/InGaAs/AlGaAs DBH was grown epitaxially, after which a cylindrical pillar was etched through the DBH. Finally, metallic contacts were made for electrical control[19] of the QD. Typical QD dimensions are a diameter of about 500 nm and a thickness of about 50 nm. The confinement potential due to the AlGaAs barriers is about 200 meV. The optical quality of VQDs is usually fairly poor due to the etched boundaries. However,

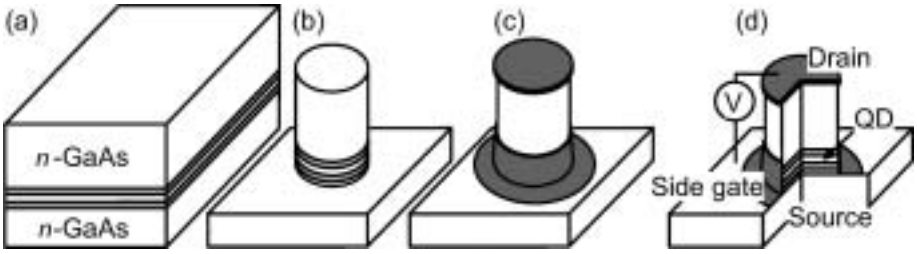

Figure 4.6 Fabrication process of a VQD consists mainly of (a) epitaxial growth of a BDH, (b) etching of a pillar through the DBH, and (c) the metallization (following Ref. 19). The QD of the device is defined by the DBH and the side gate. (d) The final device.

VQDs are attractive for electrical devices because of the well-controlled geometry and the well-defined electrical contacts.

4.2.2.2 Si quantum dots

Si QDs discussed here are lithographically defined Si islands either completely isolated by SiO_2 or connected to the environment through narrow Si channels. Si QDs can be fabricated using conventional CMOS technology on a silicon-on-insulator (SOI) wafer. The SOI wafer enables complete electrical isolation from the substrate. Figure 4.7 shows schematically the fabrication process[20] of Si QDs. A narrow wire is etched using electron beam lithography from the top Si layer. The QD is then formed in the wire by thermal oxidation. The oxidation rate is sensitive to the local O_2 influx and the local strain field. Both depend strongly on the geometry and, as a result, the center of the Si wire is oxidized very slowly compared to the rest. Therefore, the oxidation process gives rise to constrictions pinning off the wire from the leads, resulting in a Si QD in the center of the wire. This technique has been developed[21] further to fabricate double QDs and even memory and logical gate devices.[22] The main advantage of this technique is the easy integration to CMOS circuits. Si QDs do also have the potential to operate at room temperature due to very high carrier confinement ($V_C \approx 3$ eV) and small size. However, these Si QDs cannot be used for optical applications due to the low quantum efficiency of Si.

4.2.3 Field-effect quantum dots

In a FEQD, the charge carriers are confined into a 2D electron gas (2DEG) by a modulation-doped heterojunction. Within the 2DEG plane, the charges are electrostatically confined by external gates. Figure 4.8(a) shows schematically a typical device geometry, whereas Fig. 4.8(b) represents a more sophisticated double QD system. The ohmic contacts in Fig. 4.8(a) represent any kind of electric contacts to the QD. The effective potential of a FEQD is very smooth and, within the plane

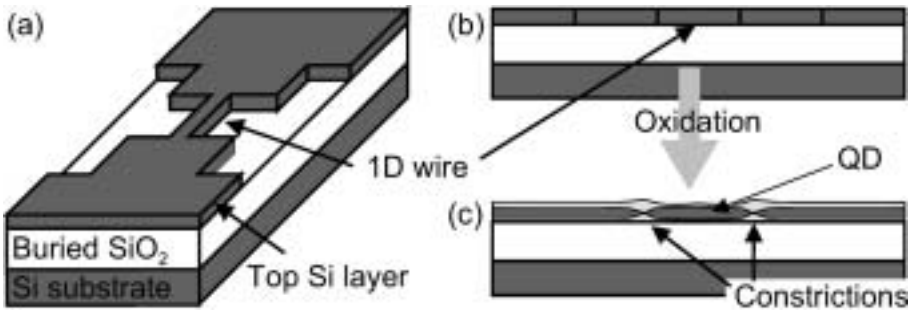

Figure 4.7 Fabrication process of a Si QD: (a) bird's eye perspective of a narrow Si wire, etched from the top Si layer of a SOI wafer; (b) cross section along the center of the wire; and (c) during thermal oxidation of the structure, the center of the wire is pinned off from the top Si layer. The result is a QD in the wire.

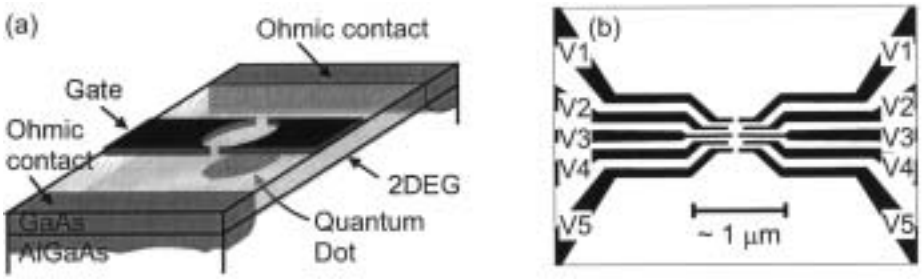

Figure 4.8 Field-induced quantum dots. (a) A schematic drawing of a FEQD in a 2DEG at the material interface between AlGaAs and GaAs. The ohmic contacts represents any electric contacts to the QD. (b) Schematic drawing of top gates of a double QD device. By using several gates, one can set the tunneling barriers (V1 and V5), the interdot tunneling coupling (V3) of multiple QDs, the number of electrons and energy levels in each QD (V4). (Reprinted with permission from Ref. 23, © 2001 The American Association for the Advancement of Science.)

of the 2DEG, its shape is close to a parabola depending on the gates. For a FEQD having a diameter around 200 nm, the spacing of the energy level is typically[23,24] tens of micro eV. These types of QDs are not expected to operate at room temperature because of the shallow potential profile. However, FEQDs are attractive for low-temperature infrared light detectors because of a very smooth gate-induced potential and high-quality heterostructure interfaces.

4.2.4 Self-assembled quantum dots

In self-assembly of QDs, one makes use of an island formation in epitaxial growth. The effect is similar to the formation of water droplets on a well-polished surface. The islands can either be QDs themselves or induce QDs in a nearby QW. The major self-assembly growth techniques are vapor phase epitaxy (VPE) and MBE.

Generally, the epitaxial growth proceeds in atomic layer-by-layer mode. However, islands are formed if there is a large lattice mismatch between the materials and/or if the surface energy of the deposited material is different from that of the substrate. The deposited material minimizes its potential energy by forming islands on the substrate. In the Stranski-Krastanow (S-K) mode, the growth starts in layer-by-layer mode and proceeds into the island mode after exceeding a critical thickness (see Fig. 4.9). Dislocation-free S-K growth has been observed in, e.g., InAs on GaAs[25] and InP on GaAs.[26] Typical island densities are 10^9 to 10^{12} cm^{-2}, depending on the growth conditions. Self-organized growth of III–V semiconductors is currently the most promising fabrication technique of optically active QDs.

4.2.4.1 Quantum dot island

The self-assembled island is a QD itself if the island is embedded in a material with a larger band gap than that of the island material. An example is provided by InAs islands in GaAs. Figure 4.10 shows QD islands schematically and a high-resolution scanning tunneling micrograph of a true InAs island. Very promising

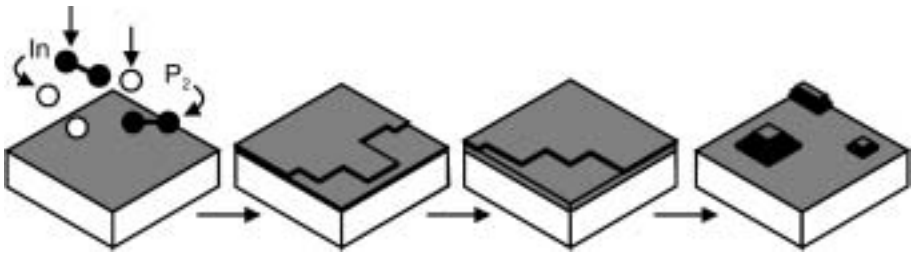

Figure 4.9 In the S-K mode, the growth of QDs starts in atomic layer-by-layer growth, but when the thickness of the overgrowth layer exceeds a critical thickness, islands begin to form.

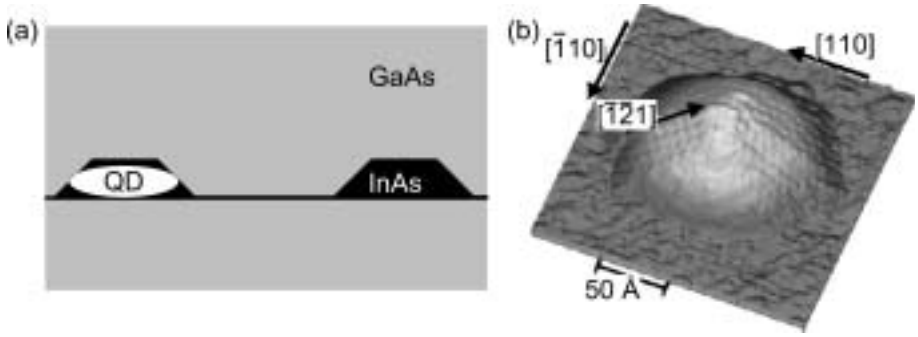

Figure 4.10 (a) Schematic image of an InAs QD island embedded in GaAs and (b) *in situ* STM image, from Ref. 29, of an InAs island.

laser structures have been fabricated using these types of quantum dots by stacking several island layers on top of each other.[27] Typical QD heights range from 5 to 15 nm and widths range from 15 to 25 nm. This means that there are very few electrons and holes per QD. The total charge confinement is a combination of strain, piezoelectric fields, and material interface effects. For a dot of 13.6 nm height, the calculated confinement energy of the electron ground state is about 180 meV.[28]

4.2.4.2 Strain-induced quantum dots

Strain is always present in self-assembled islands as well as in the substrate close to the island. The magnitude of the strain depends on the lattice constants and elastic moduli of the materials. If there is a QW close to the quantum dot, the strain field penetrates it also and affects its energy bands. The island can therefore induce a lateral carrier confinement in the QW. This results[26] in a total QD confinement in the QW. Typical stressor island heights range from 12 to 18 nm and the QW thickness is around 10 nm.[30] The lateral strain-induced confinement is very smooth and has the shape of a parabola. The strain-induced electron confinement is about 70 meV deep.[31] The resulting QD is pretty large and contains in general tens of electron-hole pairs. Figure 4.11(a) shows schematically a strain-induced QD and Fig. 4.11(b) shows a transmission electron micrograph (TEM) of self-assembled InP islands on GaAs.